Journal of Molecular Neuroscience (2022) 72:1656–1669
https://doi.org/10.1007/s12031-022-02020-y

Pharmacological Activation of GPR55 Improved Cognitive Impairment Induced by Lipopolysaccharide in Mice

Xin Wang[3] · XiaoTong Xiang[1,2] · Jie Hu[1,2] · YuMei Wu[1,2] · YueYue Li[1,2] · ShiYu Jin[1,2] · Xian Wu[1,2]

Received: 13 July 2021 / Accepted: 1 May 2022 / Published online: 20 May 2022

Abstract

Our previous research found that activation of GPR55 can alleviate cognitive impairment induced by amyloid-beta 1–42 ($A\beta_{1\text{-}42}$) and streptozotocin in mice, but the role of GPR55 in the pathogenesis of cognitive impairment remains unknown. Here, we used a lipopolysaccharide (LPS) mouse model to further investigate the role and mechanism of O-1602, a GPR55 agonist, on cognitive dysfunction. ICR mice were treated with an intracerebroventricular (i.c.v.) injection of LPS, followed by cognitive function tests. The expression of GPR55, NF-κB p65, caspase-3, Bax, and Bcl-2 in the hippocampus was examined by Western blotting. Inflammatory cytokines and microglia were detected by ELISA kit and immunohistochemical analyses, respectively. The levels of MDA, GSH, SOD, and CAT were examined by assay kits. Furthermore, TUNEL-staining was used to detect neuronal apoptosis. Our results showed that i.c.v. injection of LPS in mice exhibited impaired performance in the behavior tests, which were ameliorated by O-1602 treatment (2.0 or 4.0 μg/mouse, i.c.v.). Importantly, we found that O-1602 treatment reversed GPR55 downregulation, decreased the expression of NF-κB p65, suppressed the accumulation of proinflammatory cytokines and microglia activation, increased the anti-inflammatory cytokines, and reduced the levels of MDA, increased the levels of GSH, SOD, and CAT in the hippocampus. In addition, O-1602 treatment also significantly reduced Bax and increased Bcl-2 expression as well as decreased caspase-3 activity and TUNEL-positive cells in the hippocampus. These observations indicate that O-1602 may ameliorate LPS-induced cognition deficits via inhibiting neuroinflammation, oxidative stress, and apoptosis mediated by the NF-κB pathway in mice.

Keywords Alzheimer's disease · GPR55 · Lipopolysaccharide · Cognitive impairment

Introduction

Alzheimer's disease (AD) is a neurodegenerative disease characterized by a decline in cognitive function (Huang and Mucke 2012). The cognitive decline includes impaired working memory, long-term memory, and cognitive flexibility (Zhao et al. 2017). Previous studies have shown that neuroinflammation, oxidative stress, and apoptosis are the main processes in the development of cognitive impairment (Butterfield and Halliwell 2019; Janelidze et al. 2018; Martini et al. 2019). Furthermore, neuroinflammation and oxidative stress work together to promote cognitive dysfunction (Zhu et al. 2019). However, the exact pathogenesis of the effects of neuroinflammation, oxidative stress, and apoptosis on cognitive function remains unclear.

Lipopolysaccharide (LPS) is an endotoxin isolated from bacteria that activates the immune system, causing behavioral and memory disorders, neuroinflammation, and oxidative brain damage (Tripathi et al. 2017; Zhang et al. 2018).

Xin Wang, XiaoTong Xiang, and Jie Hu contributed equally to this work.

Highlights
- Activation of GPR55 ameliorates cognitive impairment induced by LPS in mice.
- Activation of GPR55 protects against LPS-induced neuroinflammation, oxidative stress, and apoptosis via inhibition of the NF-κB pathway in mice.
- The central GPR55 may play an important role in cognitive dysfunction.

✉ Xian Wu
wuxian2018@126.com

[1] Anhui Province Key Laboratory of Major Autoimmune Diseases, Anhui Institute of Innovative Drugs, School of Pharmacy, Anhui Medical University, Hefei 230032, China

[2] Key Laboratory of Anti-Inflammatory and Immune Medicine, Ministry of Education, Hefei 230032, China

[3] West Anhui Health Vocational College, Luan 237000, China

Previous studies have shown that intracerebroventricular (i.c.v) injection of LPS in the mouse brain has been effectively used to establish animal models of cognitive impairment (Wang et al. 2017; Zhang et al. 2018). I.c.v injection of LPS in mice produces cognitive impairment by promoting proinflammatory cytokines expression and neuronal death (Bussi et al. 2017). Moreover, the neuroinflammatory process is characterized by the activation of microglia. Microglia, the brain's resident innate immune cells, is an essential component of neuroinflammatory response (Fourrier et al. 2017). Overactivation of microglia can lead to neuronal death and the release of various neuroinflammatory mediators, such as inflammatory cytokines (Baik et al. 2019). Therefore, inhibition of microglia activation to reduce inflammatory factors is an important method for the treatment of cognitive impairment. Oxidative stress is a state in which oxidants produce an overwhelming antioxidant defense, which is associated with the development of cognitive impairment (Tonnies and Trushina 2017). Increased oxidative stress can cause damage to lipids, DNA, and proteins, leading to decreased neuronal function (Tang et al. 2019). Oxidative stress is thought to upregulate the production of Aβ peptides by inducing β- and γ-secretase activity (Gandhi and Abramov 2012). In addition, LPS induces neuroinflammation and oxidative stress–mediated neuronal apoptosis by the activation of caspase (Goel et al. 2018; You et al. 2017). Caspase-3 has been identified as a key mediator of apoptosis in neuronal cells (D'Amelio et al. 2010). The pro-apoptotic molecule Bax can induce neuronal cell death, while Bcl-2 possesses the opposite effect (Wang et al. 2020). Considerable evidence has shown that nuclear factor-κB (NF-κB) is a key transcription factor that regulates the expression of proinflammatory cytokines and the levels of oxidative stress in neurons (Gao et al. 2018). Thus, blocking NF-κB promotes cognitive function management by reducing neuroinflammation, oxidative stress, and apoptosis.

G-protein-coupled receptor 55 (GPR55) is an orphan G-protein-coupled receptor, which can be activated by endocannabinoids and lipid transmitters (Oka et al. 2007; Ryberg et al. 2007). The expression of GPR55 in mouse tissue has been reported in the nervous system including the hippocampus, though its function remains unknown (Sylantyev et al. 2013). GPR55 agonists have been shown to have a neuroprotective effect on Parkinson's disease (Celorrio et al. 2017), anxiety (Rahimi et al. 2015), and pain perception (Deliu et al. 2015). In addition, it has been reported that activation of GPR55 can strongly protect from ER stress–induced apoptosis in pancreatic β-cells (Vong et al. 2019). The research reported that O-1602, a GPR55 agonist, can decrease inflammation, improve glycemic control and energy expenditure (Lipina et al. 2019). However, it is unclear whether O-1602 can improve LPS-induced cognitive impairment in mice. Our previous studies have explored the role of GPR55 in $A\beta_{1\text{-}42}$- and streptozotocin-induced mouse models of cognitive impairment (Xiang et al. 2022a, b). Herein, we further extended our curiosity to investigate the role of GPR55 in LPS-induced cognitive deficits and neurotoxicity through drug-activated receptors, and to conclude whether the receptor could be an important target for the prevention of cognitive deficits.

Materials and Methods

Drugs and Reagents

O-1602 (5-Methyl-4-[(1R, 6R)-3-methyl-6-(1-cyclohexen-1-yl]-1, 3-benzenediol) was from Intercept Pharmaceuticals. LPS (Escherichia coli serotype 0111:B4) was from Sigma-Aldrich (St. Louis, USA). Antibodies were from several companies: anti-GPR55 from Abcam (Cambridge, USA); anti-NF-κB p65, anti-caspase-3, anti-Bcl-2, anti-Bax, and anti-β-actin from Cell Signaling Technology, Inc (MA, USA). Anti-Histone H3 from Bioworld Technology Co., Ltd (Minneapolis, USA); anti-Iba1 from Cell Signaling Technology, Inc (MA, USA). Goat anti-rabbit or anti-mouse IgG-HRP (Beyotime, Shanghai, China) was used as the secondary antibody. The nucleoprotein extraction kit was from Sangon Biotech Co., Ltd (Shanghai, China). β-actin or Histone was used as the internal control for equal loading.

Animals

Male Institute of Cancer Research (ICR) mice, aged 6-week-old and weighing between 25 and 28 g, were obtained from the Center of Laboratory Animal of Anhui Medical University. Mice were maintained under standard conditions (12-h-light/dark cycle, 07:00–19:00; ambient temperature, 22 ± 1 °C; humidity, 40%) with a sufficient supply of food and water. The National Institutes of Health Guide for the Care and Use of Laboratory Animals (NIH Publications No. 80–23, revised, 1996) was used for the experiments, and the experimental procedures were approved by the Institutional Animal Care and Use Committee (IACUC) of Anhui Medical University.

Experimental Groups and Animal Treatments

Mice were randomly divided into four groups: vehicle plus vehicle (Veh + Veh), LPS plus vehicle (LPS + Veh), LPS plus O-1602 (LPS + O-1602 2.0 μg/mouse), and LPS plus O-1602 (LPS + O-1602 4.0 μg/mouse). A single i.c.v injection of LPS (2 mg/kg) was given using the stereotaxic apparatus according to our previous report (Wu et al. 2019). Mice were anesthetized using chloral hydrate (350 mg/kg, i.p.) and immobilized on a stereotaxic instrument with a flat skull

position. The injection volume of 5 µl of LPS solution or PBS (1 µl/min) was inserted into the mediolateral at a site 1.0 mm caudal to the bregma, 1.5 mm from the midline, and 2.0 mm below the dural surface. The micropipettes were left in place for 5 min to minimize the back flux of liquid. After 3 days, PBS (5 µl) with or without O-1602 was infused into the same site. After 3 days of recovery, some of the mice were subjected to behavioral tests, and the other part of mice was subjected to biological tests. A detailed schedule of treatment and behavioral tests is shown in Fig. 1.

Behavioral Analysis

Locomotor activity was evaluated in an open field chamber. Learning and memory capacity was assessed using Morris water maze (MWM), novel object recognition (NOR), and passive avoidance tests as previously described (Wu et al. 2018).

Open Field Test

Spontaneous locomotor activity was assessed by an open field test before the MWM test (Wu et al. 2019; Zhao et al. 2017). The test was carried out in an open field chamber (72 cm × 72 cm × 36 cm). Mice were placed in the center of the open field and allowed a 5-min acclimation period. For each trial, mice were placed in a corner of the device and allowed to explore for 5 min. The total distance and the time spent in central squares were recorded by an overhead video camera.

Morris Water Maze (MWM) Test

Spatial learning and memory function were assessed by the MWM test according to our previous studies (Wu et al. 2018). The MWM consisted of a large circular black pool (120-cm diameter and 60-cm height) filled to a depth of 30 cm with water at 24 ± 2 °C. The maze was divided into four quadrants, and a clear platform (9 cm in diameter) was placed inside. A mounted flag (height, 5 cm) was fixed to the platform throughout the visible-platform trial (days 1–2). Each mouse was subjected to four training sessions every day in both visible-platform and hidden-platform (days 3–5). Mice were released into the water facing the wall of the tank from one of four separate quadrants and were allowed to find the platform within 90 s. If a mouse failed to find the platform in time, the mouse would be guided to the platform. The mouse would be left on the platform to view spatial cues for 30 s, and then returned to the cage. In the probe test (day 6, without a flag attached), the mice were allowed to swim in the water tank for 90 s without the hidden platform. The trend of the mouse to search for the platform was measured by the time spent in the target quadrant, where the platform was previously located. The number of target platform location crossings was recorded by video tracking equipment and processed by a computer equipped with an analysis-management system (ANY-maze video tracking system, stoelting Company, China).

Novel Object Recognition (NOR) Test

The recognition memory of mice was evaluated by the NOR test as described previously (Fruhauf et al. 2015; Wu et al. 2018). Mice were placed in the center of the open field chamber (72 cm × 72 cm × 36 cm). First, mice completed an acquisition trial that consisted of leaving the animals in the apparatus that contained two identical objects. Twenty-four hours later, recognition memory was assessed and a different pair of dissimilar objects (a familiar and a novel one, respectively) were presented. The time spent exploring the two objects was recorded for 5 min. Behavior was recorded by a video camera mounted vertically above the test arena and analyzed using appropriate video-tracking software (Duoyi, Shanghai, China).

Passive Avoidance Test

The passive avoidance test was carried out in a trough-shaped apparatus consisting of a white illuminated chamber

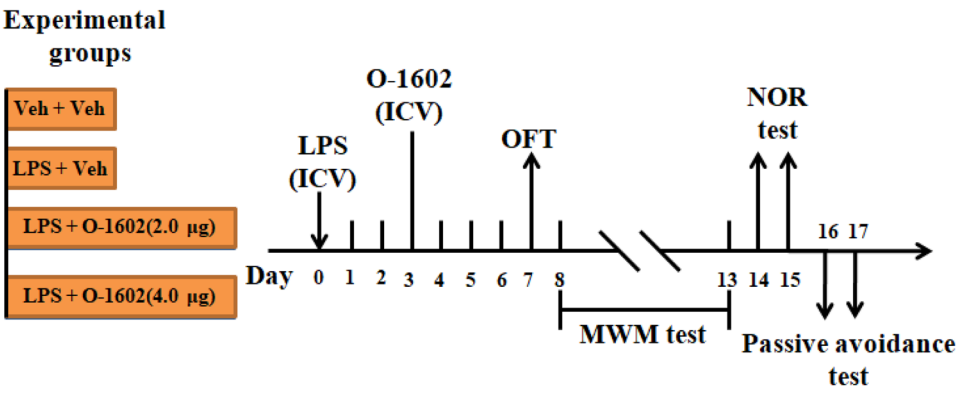

Fig. 1 Animal groups and the schedule of drug treatment and behavioral tests

and a dark chamber (20 cm × 12 cm × 60 cm, respectively). On day 1, the training trial was performed for 5 min after a 3-min adaption. When mice entered the dark chamber, an electric foot shock (40 V, 2 mA) was delivered. On day 2, the consolidation trial was performed for 5 min in the same way as training and the tracking system was started once mice were placed into the light chamber. The step-through latency and error times to enter the dark chamber were recorded (Reid et al. 2018; Wang et al. 2019).

Western Blot Analyses

Protein samples (40 μg) were added to the band and fractionated by 12% SDS-PAGE and then transferred to polyvinylidene difluoride (PVDF) membrane (Millipore). Subsequently, membranes were incubated with 5% nonfat milk containing 0.1%TBST to block nonspecific binding for 2 h at room temperature and then incubated at 4 °C overnight with respective primary antibodies for GPR55 (1:500), caspase-3(1:1000), Bcl-2(1:1000), Bax(1:500), and β-actin(1:2000), respectively, followed by incubation with horseradish peroxidase (HRP)–conjugated Goat anti-Rabbit IgG secondary antibody (1:10,000, Bioworld Technology) at room temperature for 2 h. Nuclear proteins were extracted using nucleoprotein extraction (Sangon Biotech, China). The supernatant nuclear protein extract was subjected to Western blot for NF-κB p65 (1:1000) and Histone H3 (1:500). Finally, the protein bands were visualized using an enhanced chemiluminescence kit (Synthgene Biotech, Nanjing, China). The densities of the bands were quantified by using ImageJ.

Enzyme-Linked Immunosorbent Assay (ELISA)

The homogenate was centrifuged and the supernatant was collected carefully and assayed by TNF-α, IL-1β, IL-6, and IL-10 ELISA kit (R&D Systems, Minneapolis, MN, US) according to the procedures supplied by the manufacturer (Wang et al. 2017).

Biochemical Parameter Assay

The hippocampus was rapidly dissected and homogenized. After the homogenate centrifugation, the supernatant was used to measure the levels of malondialdehyde (MDA), glutathione (GSH), superoxide dismutase (SOD), and catalase (CAT) with assay kits (Beyotime Biotechnology Institute, Nantong, China) following with the manufacturer's directions (Zhang et al. 2018).

Immunohistochemical (IHC) Analyses

The mouse brain tissue was cut into 30 μm and soaked in 3% H_2O_2 for 30 min. The brain sections were permeabilized with 0.5% Triton X-100 for 10 min and then blocked with 5% bovine serum albumin (BSA) for 1 h, and incubated with anti-iba1 (1:1000) primary antibody at 4 °C overnight. The next day, sections were incubated with biotinylated mouse anti-rabbit lgG and incubated with streptavidin–biotin complex (SABC). Diaminobenzidine (DAB) was used as the final chromogen to detect the target proteins. After gradient dehydration, sections were covered with dibutyl phthalate xylene (DPX) mounting solution and covered with glass. Photomicrographs were obtained by camera and quantified using Image-Pro Plus software. The average values of the four slices from each animal were used for statistical analysis.

TUNEL Staining

TUNEL (Terminal deoxynucleotidyl transferase (TdT)-mediated dUTP nick-end labeling) staining was performed following the instructions of the in situ cell death detection kit (Roche, Germany). The sections were fixed in 4% PFA and then washed in PBS (pH 7.4). The sections were incubated in permeabilization solution for 2 min on ice. TUNEL mixture was added to brain sections and incubated in a humidified chamber. Sections were incubated for 10 min in a dark place for DAPI staining. DAPI nuclear staining was used to determine the total number of cells in the given area. TUNEL-positive cells were determined by co-localization of the TUNEL signal and DAPI. The cells were observed with a fluorescence microscope under a fixed magnification (× 200) (Leica Microsystems AG, Germany). The number of TUNEL-positive cells in the hippocampal DG region was recorded to evaluate the neuronal apoptosis level.

Statistical Analysis

The data are shown as mean ± standard error of the mean (SEM). Group differences were analyzed by a two-way repeated measure ANOVA with "days" as the within-subject factor and "group" as the between-subject factor in the MWM test. All other data were analyzed by a one-way ANOVA followed by Dunnett's post hoc analysis for multiple comparisons. All analyses were carried out using SPSS v20.0. $P < 0.05$ was considered statistically significant.

Results

Effects of O-1602 on LPS-Treated Mice in the Open Field Test

To investigate the effects of O-1602 on spontaneous activity, mice were tested in the open field. The results showed that there was no significant difference among the groups in the total distance traveled ($F[3, 44] = 0.39$, $P = 0.71$; Fig. 2A),

and the time spent at the center (F[3, 44] = 0.24, P = 0.81; Fig. 2B), suggesting that the impaired performance was not due to a decrease in spontaneous locomotor activity.

O-1602 Ameliorates Cognitive Deficits Induced by LPS in Mice

Next, we assessed the performance of mice in the visible-platform variant (days 1–2) of the MWM test. Mice in each group exhibited similar escape latency (4 trials/mouse/day for 2 days, effect of day, F [3, 428] = 11.07, $P < 0.05$; effect of group, F [3, 428] = 1.05, $P > 0.05$; effect of group-by-day interaction, F [3, 428] = 0.07, $P > 0.05$; Fig. 3A). We then tested the mice in the spatial hidden-platform variant (days 3–5), and the data indicated that LPS treatment increased escape latency compared to the control; these were reversed by O-1602 treatment (4 trials/d for 3 d, effect of day, F [3, 620] = 13.01, $P > 0.05$; effect of group, F [3, 620] = 2.12, $P > 0.05$; effect of group-by-day interaction, F [3, 620] = 0.02, $P < 0.01$; Fig. 3B). In the probe trial (1 trial/mouse for day 6), the data indicated that the mice in the LPS + Veh group displayed a significant decrease in the percentage of time spent in the target quadrant (F[3, 44] = 5.47, $P <$ 0.01; Fig. 3C), and the number of platform location crossings (F[3, 44] = 6.38, $P < 0.01$; Fig. 3D) compared to the control, suggesting memory impairment in the LPS-treated mice. However, mice in the LPS plus O-1602 group showed significant increases in both indices compared to the LPS + Veh group (Fig. 3C and D). In addition, all the mice had similar swim speeds in the 6 days tests (Fig. 3E).

To confirm the results observed in the MWM test, we also carried out the NOR and passive avoidance tests. The NOR test was used to determine the time spent with the novel object compared with the familiar object. The discrimination index (DI) was calculated as mentioned earlier and shown in Fig. 3F reveals that the group that received LPS alone showed negative DI values, indicating non-spatial memory impairment where the mice spent more time exploring the familiar object than the novel object(F [3, 44] = 4.15, $P < 0.01$; Fig. 3F). Notably, treatment with O-1602 showed a significant increase in DI compared with the LPS + Veh group ($P < 0.05$; Fig. 3F).

Furthermore, the mice were submitted to a passive avoidance task for detecting non-spatial learning and memory. In the consolidation trial, one-way ANOVA revealed that LPS-induced cognitive deficits were observed as shorter latency (F [3, 44] = 9.37, $P < 0.01$; Fig. 3G) and more error times in the dark chamber than the control group (F [3, 44] = 7.96, $P < 0.01$; Fig. 3H). Compared with the LPS-injected group, O-1602 treatment prolonged the latency and reversed the increase in error times (Fig. 3G and H). Together, these results suggest that LPS induced cognitive impairment, specifically a deficit in memory, which can be ameliorated by O-1602 treatment.

O-1602 Reversed LPS-Induced GPR55 Downregulation in the Hippocampus

To confirm whether the protective effects of O-1602 on LPS-induced cognitive deficits were associated with GPR55, the expression of GPR55 in the hippocampus was detected by Western blot assay. Interestingly, one-way ANOVA revealed that LPS significantly reduced GPR55 expression in the hippocampus, which was reversed by O-1602 treatment (F [3, 12] = 6.78, $P < 0.01$; Fig. 4A and B). These results suggest that GPR55 might be involved in cognitive deficits induced by LPS in mice.

O-1602 Inhibits Oxidative Stress Induced by LPS in the Hippocampus

To investigate whether O-1602 has inhibitory effects on the oxidative stress induced by the i.c.v. injection of LPS in mice, we measured the levels of MDA, GSH, and the activities of SOD and CAT in the hippocampus. Our data indicated that the MDA level in the hippocampus of LPS-treated mice was significantly higher than the normal control group (F [3, 12] = 6.15, $P < 0.01$; Fig. 5A). However, the GSH level in LPS-treated mice was greatly reduced compared to

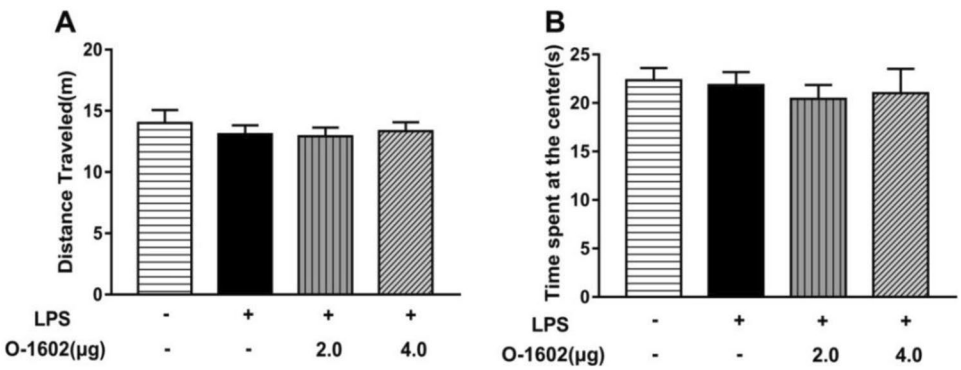

Fig. 2 Effects of O-1602 on LPS-treated mice in the open field test. (**A**) distance traveled, and (**B**) time spent in the center zone. Values shown are expressed as mean ± S.E.M; n = 10–12 mice/group

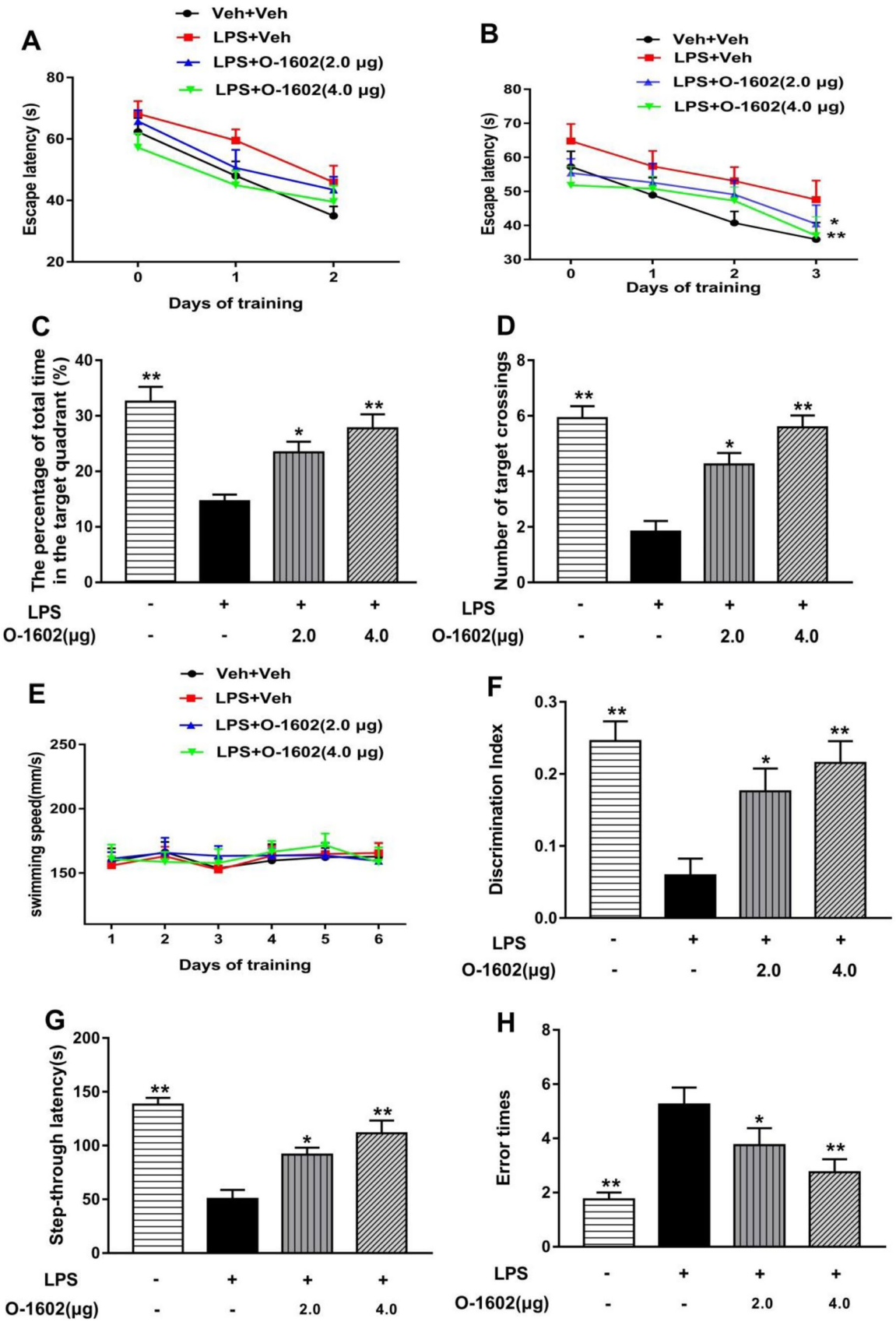
A
Veh+Veh
LPS+Veh
LPS+O-1602(2.0 μg)
LPS+O-1602(4.0 μg)
Escape latency (s)
Days of training
B
Veh+Veh
LPS+Veh
LPS+O-1602(2.0 μg)
LPS+O-1602(4.0 μg)
Escape latency (s)
Days of training
C
The percentage of total time in the target quadrant (%)
LPS
O-1602(μg)
D
Number of target crossings
LPS
O-1602(μg)
E
Veh+Veh
LPS+Veh
LPS+O-1602(2.0 μg)
LPS+O-1602(4.0 μg)
swimming speed(mm/s)
Days of training
F
Discrimination Index
LPS
O-1602(μg)
G
Step-through latency(s)
LPS
O-1602(μg)
H
Error times
LPS
O-1602(μg)

◂**Fig. 3** O-1602 ameliorates LPS-induced cognitive impairment in mice. (**A**)The mean escape latency to the visible platform. Day 0 represents the performance of the first test, and subsequent dots represent the average of all daily tests in the MWW task. (**B**) Latencies to target in the training section of the hidden platform. (**C**)Time spent in the target quadrant (%), and (**D**) numbers of platform location crossings in the probe trial test on day 6. (**E**) Average swimming speed among all groups in the 6 days tests. (**F**) The time spent on the two objects was recorded (T familiar and T novel). Results were expressed as discrimination index (DI), i.e., (T novel—T familiar)/(T familiar + T novel). The step-through latency (**G**) and error times (**H**) into the dark chamber in the consolidation trial of the passive avoidance test. The data are represented as the mean ± SEM; $n = 10–12$. $^{*}P < 0.05$, $^{**}P < 0.01$ vs. LPS + Veh group

the control group (F [3, 12] = 5.63, $P < 0.01$; Fig. 5B). Also, the SOD and CAT activities in the hippocampus of LPS-treated mice were much lower than the control group (F [3, 12] = 6.95, $P < 0.01$ for SOD, Fig. 5C; F [3, 12] = 4.81, $P < 0.01$ for CAT, Fig. 5D). After treatment, O-1602 could decrease the levels of MDA compared to the LPS-treated group, and increase the level of GSH and activities of SOD and CAT in the hippocampus.

O-1602 Inhibits Neuroinflammation in the Hippocampus Induced by LPS

To assess the ability of O-1602 to protect against LPS-induced neuroinflammation, the levels of TNF-α, IL-1β, and IL-6 in the hippocampus were detected by ELISA. One-way ANOVA revealed that the levels of TNF-α, IL-1β, and IL-6 were much higher in the LPS group compared with the control group, which was significantly suppressed by O-1602 treatment (F [3, 12] = 12.01, $P < 0.01$ for TNF-α; Fig. 6A; F [3, 12] = 14.46, $P < 0.01$ for IL-1β; Fig. 6B; F [3, 12] = 9.15, $P < 0.01$ for IL-6; Fig. 6C). Subsequently, we investigated the expression of IL-10, which is an important anti-inflammatory cytokine. The results showed that the level of IL-10 in the mice undergoing LPS administration was significantly decreased compared with the levels in the control group (F [3, 12] = 9.32, $P < 0.01$; Fig. 6D). However, O-1602 treatment could significantly increase its level in the hippocampus. These results suggest that O-1602 inhibited LPS-induced neuroinflammation in the hippocampus.

O-1602 Prevents Microglia Activation in the Hippocampus Induced by LPS

Microglia are innate immune cells in the central nervous system. When activated, microglia can synthesize and secrete a variety of cytokines, which play an important role in cognitive impairment. The results showed that LPS caused obvious microglia activation in the mouse hippocampal DG region (F [3, 12] = 5.92, $P < 0.01$ for the number of microglia cells, Fig. 7B; F [3, 12] = 6.35, $P < 0.01$ for IOD, Fig. 7C). This effect was significantly inhibited by O-1602 treatment, suggesting that O-1602 could suppress LPS-induced microglia activation in the hippocampus of the mice.

O-1602 Decreased LPS-Induced Neuronal Apoptosis in the Hippocampus

To examine whether O-1602 affected neuronal apoptosis, we performed a TUNEL assay in the hippocampal DG region of the mice. One-way ANOVA revealed that the numbers of TUNEL-positive cells in the hippocampal DG region of the LPS + Veh group were significantly higher than in the control group (F [3, 12] = 9.39, $P < 0.01$, Fig. 8B). However, O-1602 treatment decreased the number of apoptotic cells compared with the LPS + Veh group (Fig. 8B). The anti-apoptotic effects of O-1602 were further investigated by detecting apoptotic-related proteins in the hippocampus. The results showed that the expression of active caspase-3 was induced by LPS but decreased by O-1602 treatment. The expression of Bcl-2 protein was

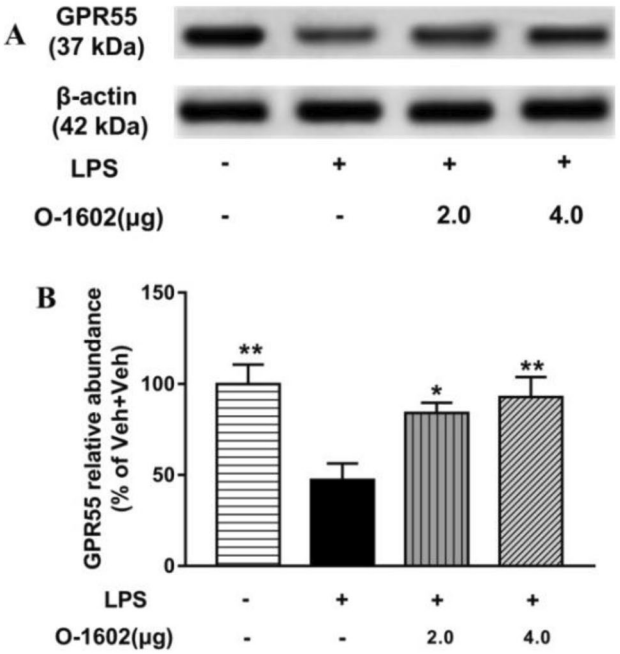

Fig. 4 GPR55 expression was downregulated by LPS exposure and reversed by O-1602 treatment. (**A**) Representative bands of GPR55 and β-actin on the gel and the expression of GPR55 normalized to that of β-actin as an internal control. (**B**) Quantification of GPR55 was expressed as the ratio (in percentage) of the Veh + Veh group. The data are represented as the mean ± SEM; $n = 4$. $^{*}P < 0.05$, $^{**}P < 0.01$ vs. LPS + Veh group

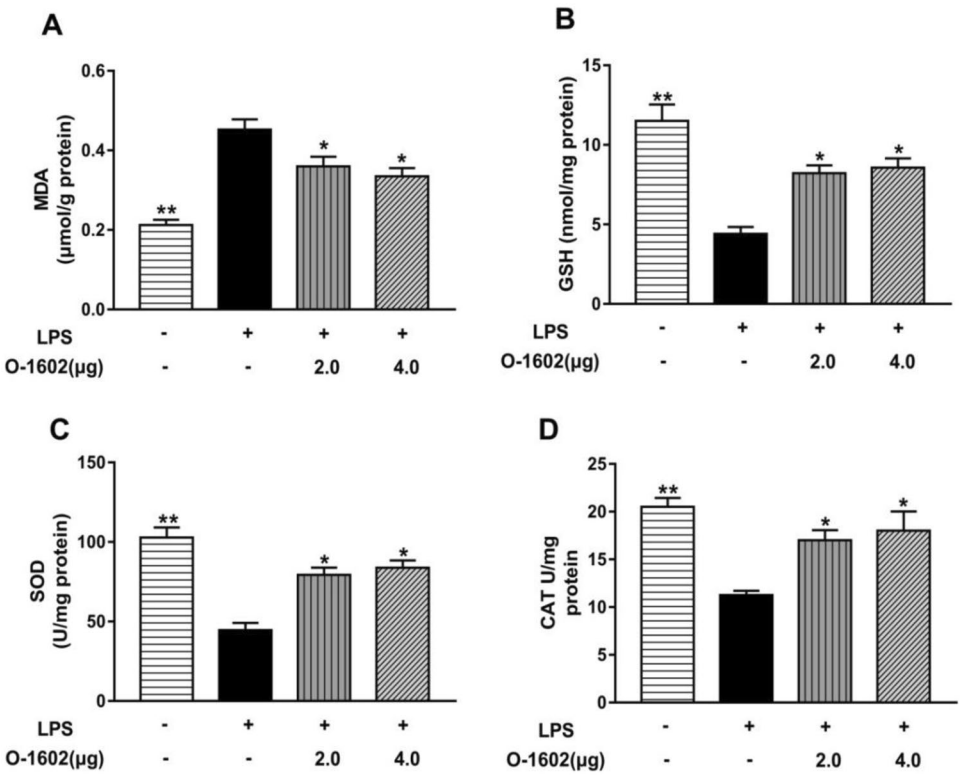

Fig. 5 O-1602 against LPS-induced oxidative stress in the hippocampus. The level of MDA (**A**), GSH (**B**), SOD (**C**), and CAT (**D**). The data are represented as the mean ± SEM; $n = 4$. $^{*}P < 0.05$, $^{**}P < 0.01$ vs. LPS + Veh group

significantly decreased in the LPS-treated mice while O-1602 treatment was able to restore Bcl-2 protein content to that comparable to the Veh + Veh group. The Bax expression was significantly less than that of LPS + Veh group, and the ratio of Bcl-2/Bax was markedly increased after O-1602 treatment (Caspase-3: F [3, 12] = 6.64, $P < 0.01$; Fig. 8D; Bcl-2/Bax: F [3, 12] = 7.94, $P < 0.01$; Fig. 8E). These data suggested that O-1602 may ameliorate the learning and memory ability by reducing LPS-induced hippocampal neuron apoptosis.

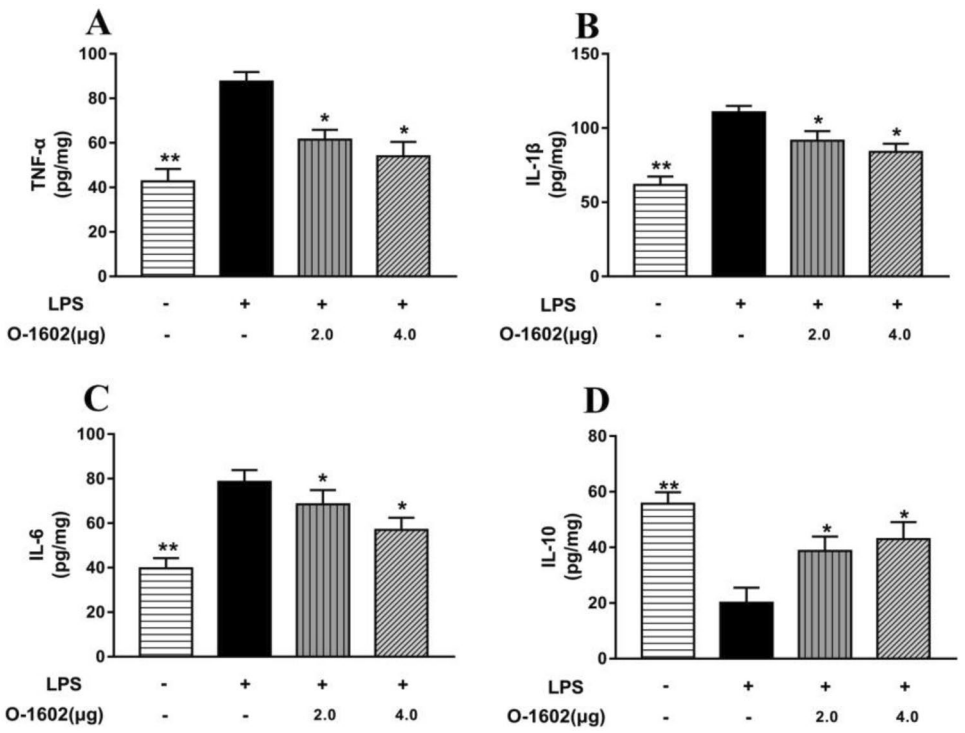

Fig. 6 O-1602 inhibited LPS-induced neuroinflammation in mice. Quantification of (**A**) TNF-α, (**B**) IL-1β, and (**C**) IL-6, (**D**) IL-10. The data are represented as the mean ± SEM; $n = 4$. $^{*}P < 0.05$, $^{**}P < 0.01$ vs. LPS + Veh group

O-1602 Suppresses LPS-Activated NF-κB Signaling in the Hippocampus

NF-κB p65 regulates many target genes involved in the immune-inflammatory response, oxidative stress, and apoptosis (Fu et al. 2019; Lei et al. 2021). To investigate whether O-1602 is associated with LPS-activated NF-κB p65 signaling, the expression of nuclear NF-κB p65 in the hippocampus was detected using the Western blot assay. Our data showed that the nuclear translocation of NF-κB p65 was significantly higher in the hippocampus of LPS-treated mice as compared with the control group. Interestingly, O-1602 treatment significantly prevented the LPS-induced increased nuclear translocation of NF-κB p65 in the hippocampus (F [3, 12] = 10.12, $P < 0.01$; Fig. 9A and B). This data suggest that inhibition of the nuclear translocation of NF-κB may be a critical mechanism by which O-1602 mediates its protective effect against LPS-induced neuroinflammation, oxidative stress, and apoptosis in mice.

Discussion

This study showed that O-1602 prevented LPS-induced cognitive deficits, including deficits in spatial learning and memory. The behavioral tests were used as robust and reliable tests that reflect hippocampal-dependent learning and memory. In the hidden platform test of MWM, the escape latency of these mice was increased after LPS exposure. For the probe test, the LPS-induced mouse model showed a significant decrease in the time spent on the target quadrant and the number of target crossings. LPS treatment also caused a significant decline in DI. In the consolidation of the passive avoidance task, LPS-induced cognitive deficits were observed as shorter latency and more error times in the dark

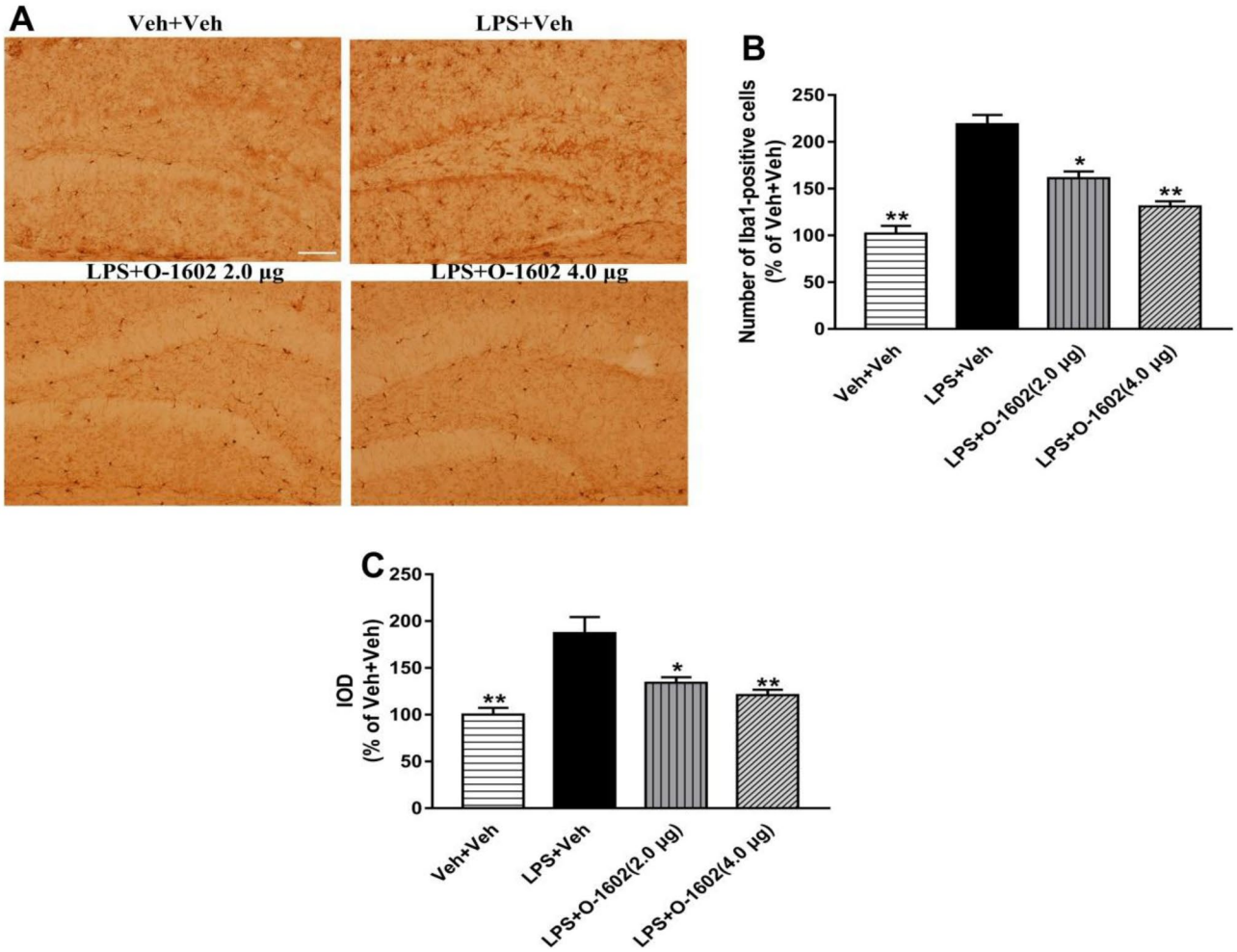

Fig. 7 O-1602 attenuates LPS-induced microglia activation in the hippocampus. (**A**) Representative images of Iba1-labeled activated microglia in the hippocampal DG region. The scale bar represents 100 μm. (**B**) Quantification of the number of Iba1-positive cells, and (**C**) IOD. The data are represented as the mean ± SEM; $n = 4$. $^{*}P < 0.05$, $^{**}P < 0.01$ vs. LPS + Veh group

chamber in the mice. In addition, LPS treatment led to memory deficit with neuroinflammation, oxidative stress, and apoptosis in mice as evidenced by increased nuclear translocation NF-κB p65, elevated pro-inflammatory cytokines, activated microglia cells, decreased anti-inflammatory cytokines, increased MDA level, and decreased the level of GSH, SOD, and CAT, and increased TUNEL-positive cells, activation of caspase-3, decreased the ratio of Bcl-2/Bax in the hippocampus. Importantly, we also found that LPS treatment decreased GPR55 expression in the hippocampus. However, O-1602 significantly inhibited such adverse cognitive and biochemical changes induced by the i.c.v. injection of LPS in mice. Overall, these suggest that O-1602 may have the potential to protect against LPS-induced cognition impairments in mice.

The GPR55 receptor can regulate energy balance and glucose homeostasis (Wargent et al. 2020). However, more attention has been given to their role in central nervous system diseases. It has been reported that GPR55 agonist exerts an anxiolytic-like effect (Wrobel et al. 2020). Most probably, GPR55 also participates in hippocampal plasticity and may play an important role in the modulation of memory and learning (Hurst et al. 2017). Increasing evidence indicates that neuroinflammation may play a crucial role in the development of memory deficits (Wu et al. 2017; Zhao et al. 2019). It has been reported that the ROS system is associated with the pathology that results from neuroinflammation (Khan et al. 2016). LPS, a stressor produced by gut microbiota, impairs memory and induces inflammatory responses in the hippocampus (Pintado et al. 2012). LPS has been widely used to study neuroinflammation-associated behavioral and pathological changes in the brain of animal models. Many studies have found i.c.v. administration of LPS in mice produces cognitive impairment by expression of pro-inflammatory cytokines and neuronal death. This method can be effectively used as an animal model for AD (Lee et al. 2017; Liu et al. 2018; Zhao et al. 2017). Our previous study found that activation of GPR55 can improve $A\beta_{1\text{-}42}$ and streptozotocin-induced neuroinflammation in mice, but it is still unclear whether it can improve LPS-induced neuroinflammation (Xiang et al. 2022a, b). Therefore, in this study, we continued to explore the functional role of GPR55 in a

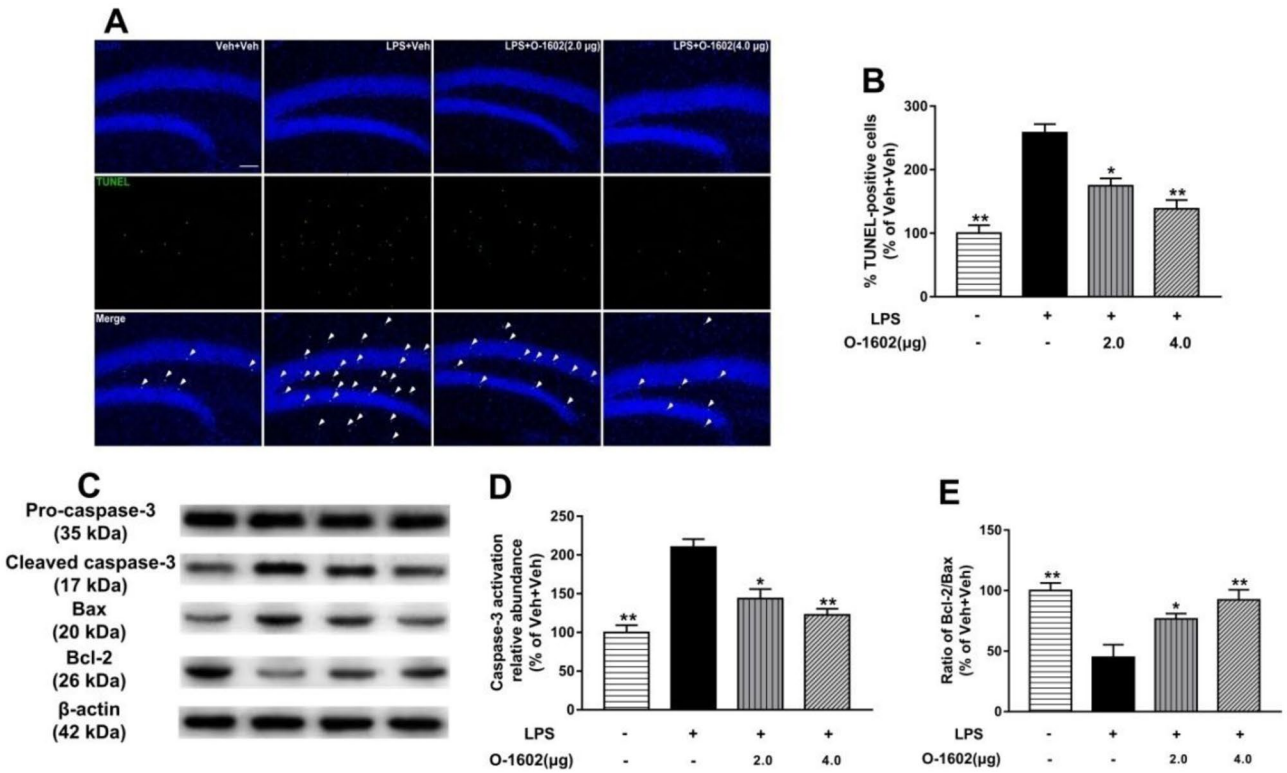

Fig. 8 O-1602 alleviates LPS-induced neuronal apoptosis in the hippocampus. (**A**) Representative images of TUNEL-positive cells in the hippocampal DG region. Scale bar = 100 μm. (**B**) The apoptotic bodies were expressed as a percentage of the total number of cells and were expressed as the ratio (in percentage) of the Veh + Veh group. (**C**) Representative bands of Pro-caspase-3, cleaved caspase-3, Bax and Bcl-2, and β-actin on the gel and the expression of pro-caspase-3, cleaved caspase-3, Bax and Bcl-2 normalized to that of β-actin as an internal control. (**D**) Caspase-3 activation was expressed as the ratio of the caspase-3 fragment to pro-caspase-3. (**E**) The ratio of Bcl-2/Bax was expressed as the ratio (in percentage) of the Veh + Veh group. The data are represented as the mean ± SEM; n = 4. $^{*}P < 0.05$, $^{**}P < 0.01$ vs. LPS + Veh group

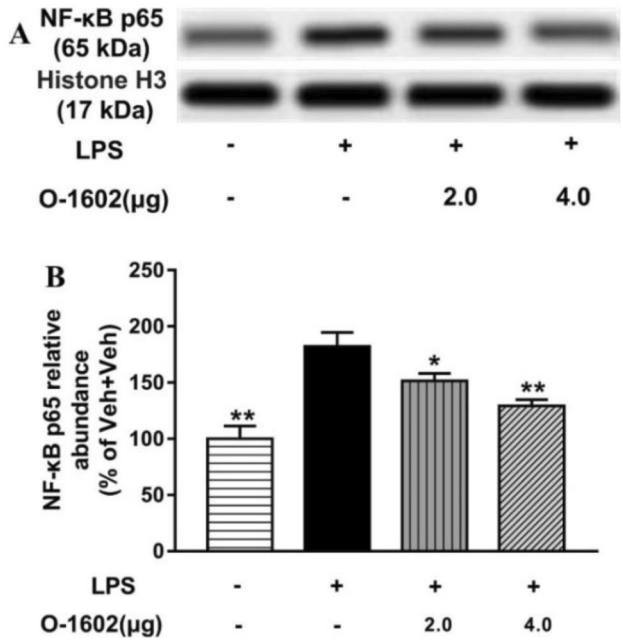

Fig. 9 O-1602 suppresses LPS-activated NF-κB signaling in the hippocampus. (**A**) NF-κB p65 and Histone H3 protein bands on the gel and the expression of NF-κB p65 normalized to that of Histone H3 as an internal control. (**B**) Quantification of NF-κB p65 was expressed as the ratio (in percentage) of the Veh + Veh group. The data are represented as the mean ± SEM; $n = 4$. $^{*}P < 0.05$, $^{**}P < 0.01$ vs. LPS + Veh group

model of LPS-induced neuroinflammation in mice. Consistent with previous studies, we found that activation of GPR55 ameliorates LPS-induced neuroinflammation in mice.

The expression of several inflammatory genes such as inflammatory cytokines can be regulated by NF-κB activation. NF-κB is an important transcription factor that is involved in pro-inflammatory gene activation as well as other gene regulations (Goel et al. 2018). Furthermore, NF-κB signaling enhances apoptosis, and inhibition of NF-κB not only protracts inflammatory responses but also prevents apoptosis. We speculate that the anti-inflammation effect of O-1602 might be mediated through the NF-κB signaling pathway. Microglia, the brain's resident immune cells, have been discovered to play an important role in neuroinflammation (Heppner et al. 2015; Unger et al. 2018). Thus, inhibition of activated microglia cells can help to ameliorate the severity of neuroinflammation. In this study, O-1602 treatment improved neuroinflammation by inhibiting inflammatory signaling molecule (NF-κB p65) and the microglia activation in the hippocampus of LPS-exposed mice.

Activated microglia are the major source of ROS in the brain (Block et al. 2007). To detect oxidative stress during neuroinflammation induced by LPS and to verify the antioxidative effect of O-1602, we measured the level of MDA and GSH, and the activities of SOD and CAT in the hippocampus. In this study, treatment with O-1602 attenuated the LPS-induced increase in MDA and decrease in the activities of SOD and CAT and the level of GSH in the hippocampus. This result agrees with the evidence that suggests that ROS-induced oxidative stress is one of the most common toxic mechanisms. Furthermore, ROS is capable of modulating gene expression. ROS may trigger the generation of cytokines and participate in inflammatory signaling.

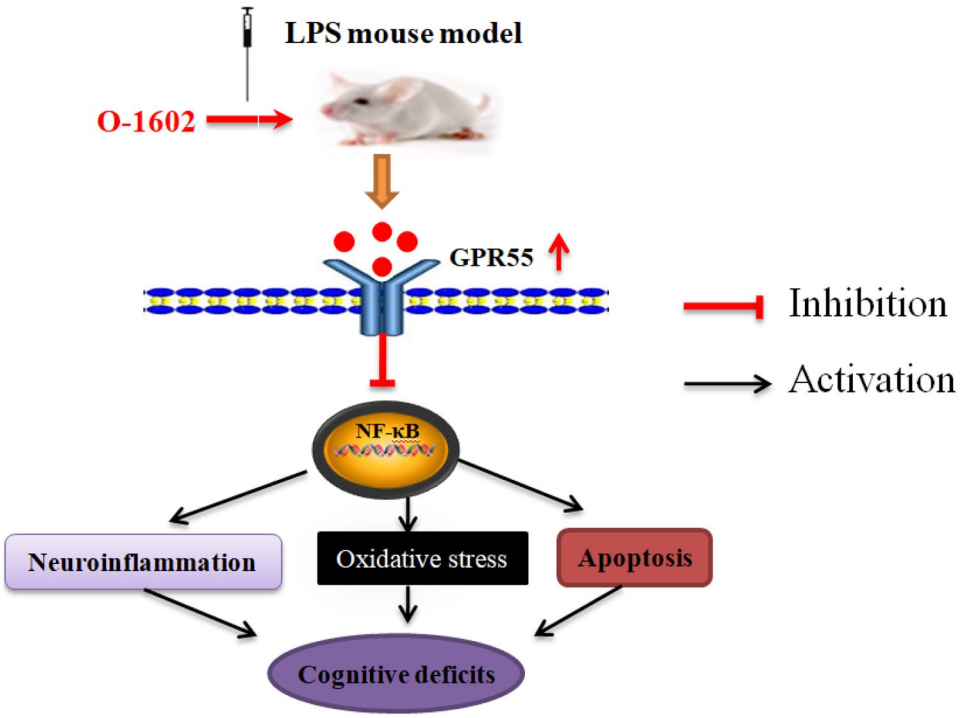

Fig. 10 Schematic representation illustrating the mechanism of O-1602 on its neuroprotective effects

In addition, NF-κB is central to the acquisition of the pro-inflammatory phenotype, and it is particularly sensitive to ROS (Zhang et al. 2018). It has been reported that GPR55 expression was observed in microglia (Saliba et al. 2018), and inhibition of NF-κB transcriptional activity in the microglia nucleus suppressed proinflammatory cytokine expression. Thus, our results demonstrated that O-1602 attenuated inflammatory oxidative stress.

Previous studies have shown that apoptosis plays an important role in the progression of AD (Gandhi and Abramov 2012; Lei et al. 2021). LPS-induced neuroinflammation enhances apoptotic neurodegeneration (Lee et al. 2013). Early cell changes that occur during apoptosis are mediated by the Bcl-2 family of proteins, including the anti-apoptotic Bcl-2 and pro-apoptotic Bax (Goel et al. 2018). Caspase-3 is considered to be an important feature of apoptosis in neuronal cells. Activation of caspase-3 leads to the death of neuronal cells (Clark et al. 2000). In this study, the results are consistent with previous findings. Our results showed that after exposure to LPS, the expression of Bcl-2 protein decreased; while the expression of Bax increased. Furthermore, treatment with O-1602 downregulated the expression of Bax and upregulated the expression of Bcl-2, and mitigated caspase 3 activity and the number of apoptotic cells in LPS-treated mice. The results suggest that O-1602 may improve cognitive dysfunction by reducing LPS-induced neuronal apoptosis in the hippocampus.

Conclusion

In summary, as shown in Fig. 10, our study indicates that GPR55 agonist O-1602 displays neuroprotective effects on LPS-induced memory impairment, neuroinflammation, oxidative stress, and apoptosis via inhibition of the NF-κB pathway in mice. Combined with our previous studies, we speculate that GPR55 may be a potential regulator of AD-related phenotypes, and suggest that this receptor may be a therapeutic target for the prevention and treatment of AD.

Author Contribution XW conceived and designed the study. XTX, JH, YMW, YYL, and SYJ performed the experiments and collected the data. XW analyzed the data, and drafted this article. All authors read and approved the final manuscript.

Funding This project was supported by the Natural Science Foundation of Anhui Province (2108085QH385), Doctor Foundation of Anhui Medical University (0601086201), Anhui Medical University School Funding Project (2020xkj012), and National undergraduate innovation and entrepreneurship training program (202010366022).

Data Availability We declared that materials described in the manuscript, including all relevant raw data, will be freely available to any scientist wishing to use them for non-commercial purposes, without breaching participant confidentiality.

Declarations

Ethics Approval and Consent to Participate The studies involving animals were approved and performed in accordance with the ethical standards of the institutional animal ethics committee in Anhui Medical University.

Consent for Publication All authors have seen the manuscript and given their consent for publication.

Conflict of Interest The authors declare no competing interests.

References

Baik SH, Kang S, Lee W, Choi H, Chung S, Kim JI, Mook-Jung I (2019) A breakdown in metabolic reprogramming causes microglia dysfunction in Alzheimer's disease. Cell Metab 30:493–507

Block ML, Zecca L, Hong JS (2007) Microglia-mediated neurotoxicity: uncovering the molecular mechanisms. Nat Rev Neurosci 8:57–69

Bussi C, Peralta Ramos JM, Arroyo DS, Gaviglio EA, Gallea JI, Wang JM, Celej MS, Iribarren P (2017) Autophagy down regulates pro-inflammatory mediators in BV2 microglial cells and rescues both LPS and alpha-synuclein induced neuronal cell death. Sci Rep 7:43153

Butterfield DA, Halliwell B (2019) Oxidative stress, dysfunctional glucose metabolism and Alzheimer disease. Nat Rev Neurosci 20:148–160

Celorrio M, Rojo-Bustamante E, Fernandez-Suarez D, Saez E, Estella-Hermoso de Mendoza A, Muller CE, Ramirez MJ, Oyarzabal J, Franco R, Aymerich MS (2017) GPR55: a therapeutic target for Parkinson's disease? Neuropharmacology 125:319–332

Clark RS, Kochanek PM, Watkins SC, Chen M, Dixon CE, Seidberg NA, Melick J, Loeffert JE, Nathaniel PD, Jin KL, Graham SH (2000) Caspase-3 mediated neuronal death after traumatic brain injury in rats. J Neurochem 74:740–753

D'Amelio M, Cavallucci V, Cecconi F (2010) Neuronal caspase-3 signaling: not only cell death. Cell Death Differ 17:1104–1114

Deliu E, Sperow M, Console-Bram L, Carter RL, Tilley DG, Kalamarides DJ, Kirby LG, Brailoiu GC, Brailoiu E, Benamar K, Abood ME (2015) The lysophosphatidylinositol receptor GPR55 modulates pain perception in the periaqueductal gray. Mol Pharmacol 88:265–272

Fourrier C, Remus-Borel J, Greenhalgh AD, Guichardant M, Bernoud-Hubac N, Lagarde M, Joffre C, Laye S (2017) Docosahexaenoic acid-containing choline phospholipid modulates LPS-induced neuroinflammation in vivo and in microglia in vitro. J Neuroinflammation 14:170

Fruhauf PK, Ineu RP, Tomazi L, Duarte T, Mello CF, Rubin MA (2015) Spermine reverses lipopolysaccharide-induced memory deficit in mice. J Neuroinflammation 12:3

Fu L, Liu C, Chen L, Lv Y, Meng G, Hu M, Long Y, Hong H, Tang S (2019) Protective effects of 1-methylnicotinamide on Abeta1-42-induced cognitive deficits, neuroinflammation and apoptosis in mice. J Neuroimmune Pharmacol 14:401–412

Gandhi S, Abramov AY (2012) Mechanism of oxidative stress in neurodegeneration. Oxid Med Cell Longev 2012:428010

Gao J, Xiong B, Zhang B, Li S, Huang N, Zhan G, Jiang R, Yang L, Wu Y, Miao L, Zhu B, Yang C, Luo A (2018) Sulforaphane alleviates lipopolysaccharide-induced spatial learning and memory

dysfunction in mice: the role of BDNF-mTOR signaling pathway. Neuroscience 388:357–366
Goel R, Bhat SA, Hanif K, Nath C, Shukla R (2018) Angiotensin II receptor blockers attenuate lipopolysaccharide-induced memory impairment by modulation of NF-kappaB-mediated BDNF/CREB expression and apoptosis in spontaneously hypertensive rats. Mol Neurobiol 55:1725–1739
Heppner FL, Ransohoff RM, Becher B (2015) Immune attack: the role of inflammation in Alzheimer disease. Nat Rev Neurosci 16:358–372
Huang Y, Mucke L (2012) Alzheimer mechanisms and therapeutic strategies. Cell 148:1204–1222
Hurst K, Badgley C, Ellsworth T, Bell S, Friend L, Prince B, Welch J, Cowan Z, Williamson R, Lyon C, Anderson B, Poole B, Christensen M, McNeil M, Call J, Edwards JG (2017) A putative lysophosphatidylinositol receptor GPR55 modulates hippocampal synaptic plasticity. Hippocampus 27:985–998
Janelidze S, Mattsson N, Stomrud E, Lindberg O, Palmqvist S, Zetterberg H, Blennow K, Hansson O (2018) CSF biomarkers of neuroinflammation and cerebrovascular dysfunction in early Alzheimer disease. Neurology 91:e867–e877
Khan MS, Ali T, Kim MW, Jo MH, Jo MG, Badshah H, Kim MO (2016) Anthocyanins protect against LPS-induced oxidative stress-mediated neuroinflammation and neurodegeneration in the adult mouse cortex. Neurochem Int 100:1–10
Lee HJ, Lim SM, Ko DB, Jeong JJ, Hwang YH, Kim DH (2017) Soyasapogenol B and genistein attenuate lipopolysaccharide-induced memory impairment in mice by the modulation of NF-kappaB-mediated BDNF expression. J Agric Food Chem 65:6877–6885
Lee YJ, Choi DY, Yun YP, Han SB, Oh KW, Hong JT (2013) Epigallocatechin-3-gallate prevents systemic inflammation-induced memory deficiency and amyloidogenesis via its anti-neuroinflammatory properties. J Nutr Biochem 24:298–310
Lei S, Wu S, Wang G, Li B, Liu B, Lei X (2021) Pinoresinol diglucoside attenuates neuroinflammation, apoptosis and oxidative stress in a mice model with Alzheimer's disease. NeuroReport 32:259–267
Lipina C, Walsh SK, Mitchell SE, Speakman JR, Wainwright CL, Hundal HS (2019) GPR55 deficiency is associated with increased adiposity and impaired insulin signaling in peripheral metabolic tissues. FASEB J 33:1299–1312
Liu Y, Zhang Y, Zheng X, Fang T, Yang X, Luo X, Guo A, Newell KA, Huang XF, Yu Y (2018) Galantamine improves cognition, hippocampal inflammation, and synaptic plasticity impairments induced by lipopolysaccharide in mice. J Neuroinflammation 15:112
Martini F, Rosa SG, Klann IP, Fulco BCW, Carvalho FB, Rahmeier FL, Fernandes MC, Nogueira CW (2019) A multifunctional compound ebselen reverses memory impairment, apoptosis and oxidative stress in a mouse model of sporadic Alzheimer's disease. J Psychiatr Res 109:107–117
Oka S, Nakajima K, Yamashita A, Kishimoto S, Sugiura T (2007) Identification of GPR55 as a lysophosphatidylinositol receptor. Biochem Biophys Res Commun 362:928–934
Pintado C, Gavilan MP, Gavilan E, Garcia-Cuervo L, Gutierrez A, Vitorica J, Castano A, Rios RM, Ruano D (2012) Lipopolysaccharide-induced neuroinflammation leads to the accumulation of ubiquitinated proteins and increases susceptibility to neurodegeneration induced by proteasome inhibition in rat hippocampus. J Neuroinflammation 9:87
Rahimi A, Hajizadeh Moghaddam A, Roohbakhsh A (2015) Central administration of GPR55 receptor agonist and antagonist modulates anxiety-related behaviors in rats. Fundam Clin Pharmacol 29:185–190
Reid SNS, Ryu JK, Kim Y, Jeon BH (2018) GABA-enriched fermented Laminaria japonica improves cognitive impairment and neuroplasticity in scopolamine- and ethanol-induced dementia model mice. Nurs Res Pract 12:199–207
Ryberg E, Larsson N, Sjogren S, Hjorth S, Hermansson NO, Leonova J, Elebring T, Nilsson K, Drmota T, Greasley PJ (2007) The orphan receptor GPR55 is a novel cannabinoid receptor. Br J Pharmacol 152:1092–1101
Saliba SW, Jauch H, Gargouri B, Keil A, Hurrle T, Volz N, Mohr F, van der Stelt M, Brase S, Fiebich BL (2018) Anti-neuroinflammatory effects of GPR55 antagonists in LPS-activated primary microglial cells. J Neuroinflammation 15:322
Sylantyev S, Jensen TP, Ross RA, Rusakov DA (2013) Cannabinoid- and lysophosphatidylinositol-sensitive receptor GPR55 boosts neurotransmitter release at central synapses. Proc Natl Acad Sci USA 110:5193–5198
Tang J, Diao P, Shu X, Li L, Xiong L (2019) Quercetin and quercitrin attenuates the inflammatory response and oxidative stress in LPS-Induced RAW264.7 cells: in vitro assessment and a theoretical model. BioMed Res Int 2019:7039802
Tonnies E, Trushina E (2017) Oxidative stress, synaptic dysfunction, and Alzheimer's disease. J Alzheimer's Dis 57:1105–1121
Tripathi A, Paliwal P, Krishnamurthy S (2017) Piracetam attenuates LPS-induced neuroinflammation and cognitive impairment in rats. Cell Mol Neurobiol 37:1373–1386
Unger MS, Schernthaner P, Marschallinger J, Mrowetz H, Aigner L (2018) Microglia prevent peripheral immune cell invasion and promote an anti-inflammatory environment in the brain of APP-PS1 transgenic mice. J Neuroinflammation 15:274
Vong CT, Tseng HHL, Kwan YW, Lee SM, Hoi MPM (2019) Novel protective effect of O-1602 and abnormal cannabidiol, GPR55 agonists, on ER stress-induced apoptosis in pancreatic beta-cells. Biomed Pharmacother 111:1176–1186
Wang LS, Tao X, Liu XM, Zhou YF, Zhang MD, Liao YH, Pan RL, Chang Q (2019) Cajaninstilbene acid ameliorates cognitive impairment induced by intrahippocampal injection of amyloid-beta1-42 oligomers. Front Pharmacol 10:1084
Wang Y, Gu J, Hu L, Kong L, Wang T, Di M, Li C, Gui S (2020) miR-130a alleviates neuronal apoptosis and changes in expression of Bcl-2/Bax and caspase-3 in cerebral infarction rats through PTEN/PI3K/Akt signaling pathway. Exp Ther Med 19:2119–2126
Wang YW, Zhou Q, Zhang X, Qian QQ, Xu JW, Ni PF, Qian YN (2017) Mild endoplasmic reticulum stress ameliorates lipopolysaccharide-induced neuroinflammation and cognitive impairment via regulation of microglial polarization. J Neuroinflammation 14:233
Wargent ET, Kepczynska M, Zaibi MS, Hislop DC, Arch JRS, Stocker CJ (2020) High fat-fed GPR55 null mice display impaired glucose tolerance without concomitant changes in energy balance or insulin sensitivity but are less responsive to the effects of the cannabinoids rimonabant or Delta(9)-tetrahydrocannabivarin on weight gain. PeerJ 8:e9811
Wrobel A, Serefko A, Szopa A, Ulrich D, Poleszak E, Rechberger T (2020) O-1602, an agonist of atypical cannabinoid receptors GPR55, reverses the symptoms of depression and detrusor overactivity in rats subjected to corticosterone treatment. Front Pharmacol 11:1002
Wu H, Wang X, Gao J, Liang S, Hao Y, Sun C, Xia W, Cao Y, Wu L (2017) Fingolimod (FTY720) attenuates social deficits, learning and memory impairments, neuronal loss and neuroinflammation in the rat model of autism. Life Sci 173:43–54
Wu X, Lv YG, Du YF, Chen F, Reed MN, Hu M, Suppiramaniam V, Tang SS, Hong H (2018) Neuroprotective effects of INT-777 against Abeta1-42-induced cognitive impairment, neuroinflammation, apoptosis, and synaptic dysfunction in mice. Brain Behav Immun 73:533–545

Wu X, Lv YG, Du YF, Hu M, Reed MN, Long Y, Suppiramaniam V, Hong H, Tang SS (2019) Inhibitory effect of INT-777 on lipopolysaccharide-induced cognitive impairment, neuroinflammation, apoptosis, and synaptic dysfunction in mice. Prog Neuropsychopharmacol Biol Psychiatry 88:360–374

Xiang X, Wang X, Jin S, Hu J, Wu Y, Li Y, Wu X (2022a) Activation of GPR55 attenuates cognitive impairment and neurotoxicity in a mouse model of Alzheimer's disease induced by Abeta1-42 through inhibiting RhoA/ROCK2 pathway. Prog Neuropsychopharmacol Biol Psychiatry 112:110423

Xiang X, Wang X, Wu Y, Hu J, Li Y, Jin S, Wu X (2022b) Activation of GPR55 attenuates cognitive impairment, oxidative stress, neuroinflammation, and synaptic dysfunction in a streptozotocin-induced Alzheimer's mouse model. Pharmacol Biochem Behav 214:173340

You LH, Yan CZ, Zheng BJ, Ci YZ, Chang SY, Yu P, Gao GF, Li HY, Dong TY, Chang YZ (2017) Astrocyte hepcidin is a key factor in LPS-induced neuronal apoptosis. Cell Death Dis 8:e2676

Zhang XY, Xu ZP, Wang W, Cao JB, Fu Q, Zhao WX, Li Y, Huo XL, Zhang LM, Li YF, Mi WD (2018) Vitamin C alleviates LPS-induced cognitive impairment in mice by suppressing neuroinflammation and oxidative stress. Int Immunopharmacol 65:438–447

Zhao WX, Zhang JH, Cao JB, Wang W, Wang DX, Zhang XY, Yu J, Zhang YY, Zhang YZ, Mi WD (2017) Acetaminophen attenuates lipopolysaccharide-induced cognitive impairment through antioxidant activity. J Neuroinflammation 14:17

Zhao Y, Deng H, Li K, Wang L, Wu Y, Dong X, Wang X, Chen Y, Xu Y (2019) Trans-cinnamaldehyde improves neuroinflammation-mediated NMDA receptor dysfunction and memory deficits through blocking NF-kappaB pathway in presenilin1/2 conditional double knockout mice. Brain Behav Immun 82:45–62

Zhu X, Liu J, Chen S, Xue J, Huang S, Wang Y, Chen O (2019) Isoliquiritigenin attenuates lipopolysaccharide-induced cognitive impairment through antioxidant and anti-inflammatory activity. BMC Neurosci 20:41